Global Optimization of Microwave Circuits Using Dimensionality Reduction and Multi-Fidelity EM Simulations

Slawomir Koziel[1,2][0000-0002-9063-2647], Anna Pietrenko-Dabrowska[2][0000-0003-2319-6782], and Leifur Leifsson[3][0000-0001-5134-870X]

[1] Engineering Optimization & Modeling Center, Department of Engineering, Reykjavík University, Menntavegur 1, 102 Reykjavík, Iceland
koziel@ru.is

[2] Faculty of Electronics Telecommunications and Informatics, Gdansk University of Technology, Narutowicza 11/12, 80-233 Gdansk, Poland
anna.dabrowska@pg.edu.pl

[3] School of Aeronautics and Astronautics, Purdue University, West Lafayette, IN 47907, USA
leifur@purdue.edu

Abstract. The growing complexity of contemporary microwave circuits made numerical optimization imperative as a performance-boosting tool. Yet, it is intricate because of the high costs incurred by electromagnetic (EM) analysis required to evaluate the system's quality reliably. These expenses are particularly significant in global optimization, which is necessary in many situations. This study introduces an innovative strategy for high-efficacy globalized optimization of passive components. Our methodology leverages reduction of the problem dimensionality implemented using a rapid global sensitivity analysis and a custom-developed machine learning (ML) algorithm employing fast surrogate models established in the reduced domain. The designs rendered by the ML process are further refined in the local sense in the full-dimensionality parameter space using a gradient-based routine. Additional improvement in efficiency is obtained by employing multi-fidelity EM simulations with the low-fidelity models used for global search and high-fidelity ones only utilized in fine-tuning. The presented approach has been comprehensively validated utilizing two coupling circuits and juxtaposed against a pool of benchmark algorithms. The obtained results underscore the remarkable efficacy of our procedure. The typical running cost does not exceed a hundred high-fidelity EM analyses, corresponding to sizable savings over the benchmark. At the same time, the proposed method renders designs of competitive quality.

Keywords: Computer-aided design, microwave engineering, optimization, EM-driven design, dimensionality reduction, multi-fidelity simulations.

ICCS Camera Ready Version 2025
To cite this paper please use the final published version:
DOI: 10.1007/978-3-031-97632-2_7

1 Introduction

Microwave passive components have become increasingly complex in fulfilling performance demands associated with emerging application areas. On top of meeting strict requirements concerning electrical characteristics [1], [2], one of the crucial considerations nowadays is miniaturization [3]. Size reduction can be achieved through appropriate geometry modifications (e.g., line folding and utilization of metamaterials [4], [5]), which lead to the further increase of topological sophistication. Accurate assessment of such circuits requires electromagnetic (EM) simulation because conventional methods, such as equivalent network modeling, cannot quantify phenomena such as cross-coupling, dielectric losses, or the effects of the system's environment (e.g., connectors, housing) [6].

Although EM-driven design is imperative, at least at the later stages of the circuit development process [7], it is also intricate. The major issues include handling multiple decision variables, design objectives, and constraints. At the same time, repetitive EM simulations incur considerable computational expenses, which is especially problematic when using numerical optimization methods. Employing the latter also requires an appropriate background and familiarity with optimization algorithms, which microwave engineers often lack. Consequently, traditional approaches relying on combining engineering insight and parametric studies are still widely used even though they cannot yield optimum results. Nonetheless, such interactive techniques are immensely laborious. Another challenge is that in a growing number of cases, global optimization is necessary to address the design problem's multimodality (e.g., design of metasurfaces, array pattern synthesis, etc. [8], [9]), unavailability of a good starting point [10], or optimization-driven miniaturization [11].

Today, global optimization is mainly conducted with nature-inspired algorithms [12], [13]. These methods leverage the exchange of information between sets of candidate solutions processed during the optimization run and the employment of stochastic components [14] to allow escaping from local optima. The literature is replete with specific procedures (e.g., [15]-[17]). Their popularity stems from straightforward handling and accessibility. Unfortunately, direct optimization of EM simulation models through population-based methods incurs tremendous computational expenses. In practice it is typically attempted if cheaper (e.g., analytical) models are available [18]. Cost-related difficulties may be alleviated with the help of surrogate modeling [19], often incorporated into machine learning (ML) frameworks [20], [21]. The ML process renders candidate solutions (infill points) using a metamodel as a fast predictor, subsequently refined using accumulated EM data [22]. Despite its potential benefits, the construction of a reliable surrogate is the most severe bottleneck of ML, mainly due to the curse of dimensionality. Mitigation methods include domain confinement [23], variable-fidelity approaches [24], feature-based methods [25], [26], and physics-based frameworks (e.g., space mapping [27]). Unfortunately, many of these solutions lack the generality and are challenging to integrate with global search engines.

This research introduces a new approach to reduced-cost globalized optimization of microwave circuits. We focus on enhancing the efficiency and reliability of the search procedure. To pursue this goal, a fast machine learning algorithm is introduced that incorporates kriging metamodels built in a dimensionality-reduced subspace. The latter

ICCS Camera Ready Version 2025
To cite this paper please use the final published version:
DOI: 10.1007/978-3-031-97632-2_7

is determined with the help of a rapid global sensitivity analysis (RGSA), which identifies directions corresponding to the most prominent changes in the system's frequency characteristics. The candidate solutions are rendered by a particle swarm optimizer (PSO) used as a core search algorithm. Cost efficiency is further enhanced by involving low-resolution EM analysis for global search. Meanwhile, the dependability is ensured by employing high-fidelity EM models at the final (gradient-based) tuning stage. Extensive numerical verification demonstrates the exquisite efficacy of our method. It is superior over several benchmark techniques, among others nature-inspired and machine-learning routines. The average cost does not exceed a hundred high-fidelity EM analyses. Meanwhile, multiple runs of the algorithm corroborate the ability of the framework to yield satisfactory results in each instance.

2 Fast Microwave Optimization by Dimensionality Reduction

Here, we elucidate the operation of the suggested global optimization procedure. The design task statement is recalled in Section 2.1. Variable-resolution EM models and rapid sensitivity analysis are discussed in Sections 2.2 and 2.3. Sections 2.4 and 2.5 elucidate the global and local search stages. Finally, Section 2.6 puts together the operation of the entire algorithm.

2.1 Problem Statement

We aim to reduce a merit function $U(\boldsymbol{x})$ encoding the design quality. Here, $\boldsymbol{x} = [x_1 \ldots x_n]^T$ represents the decision variables (here, geometry parameters of the circuit). The task is stated as

$$\boldsymbol{x}^* = \arg\min_{\boldsymbol{x}\in X} U(\boldsymbol{x}) \tag{1}$$

in which X is the search domain. The circuit outputs (scattering parameters versus frequency) are evaluated using EM analysis and denoted as $S_{ij}(\boldsymbol{x},f)$, with i and j being the indices of the port indices; f stands for the frequency. A representative example is a microwave coupler designed to enhance return loss and port isolation at a target frequency f_0. At the same time, we aim to maintain a target power division ratio K_P at f_0. The merit function may take the form of

$$U(\boldsymbol{x}) = \max\left\{|S_{11}(\boldsymbol{x},f_0)|,|S_{41}(\boldsymbol{x},f_0)|\right\} + \beta\left[|S_{21}(\boldsymbol{x},f_0)| - |S_{31}(\boldsymbol{x},f_0)| - K_P\right]^2 \tag{2}$$

In (2), the second part is a regularization factor that enforces the power division condition.

2.2 Multi-Fidelity EM Models

Multi-fidelity models have been utilized in microwave engineering for over two decades to accelerate design procedures [28]. The idea is to trade-off accuracy for speed under controlled conditions, i.e., appropriate enhancement of the low-resolution model.

ICCS Camera Ready Version 2025
To cite this paper please use the final published version:
DOI: 10.1007/978-3-031-97632-2_7

Although the less reliable representation is typically an equivalent network, it is of limited generality. In this work, we implement the low-resolution model $\boldsymbol{R}_c(\boldsymbol{x})$ by reducing the resolution of the EM analysis (i.e., using coarse discretization of the simulated circuit). This versatile approach ensures a sufficient correlation with the high-resolution model $\boldsymbol{R}_f(\boldsymbol{x})$ [29]. A representative example and typical relationship between $\boldsymbol{R}_c$ and $\boldsymbol{R}_f$ have been showcased in Fig. 1.

This study employs $\boldsymbol{R}_c$ to execute sensitivity analysis, construct the initial surrogate model (Section 2.3), and carry out the global search stage (Section 2.4). In contrast, $\boldsymbol{R}_f$ is for final tuning (Section 2.5). Note that due to a good correlation between the models (cf. Fig. 1), $\boldsymbol{R}_c$ can be used uncorrected, also because possible inaccuracies will be rectified at the last stage.

2.3 Global Sensitivity Analysis. Dimensionality-Reduced Search Domain

This study uses a surrogate-assisted ML scheme to conduct the global search stage. The major challenge is building a reliable data-driven metamodel. Here, it is facilitated through dimensionality reduction implemented using a rapid global sensitivity analysis (RGSA) adopted from [30] and outlined in Fig. 2. RGSA produces a set of orthonormal directions $\boldsymbol{e}_j$ ordered regarding their effect on the circuit response variability. These effects are quantified by the eigenvalues $\lambda_1 \geq \lambda_2 \geq \ldots \geq \lambda_n$. The restricted domain is then established using a small number N_d of the most relevant vectors collectively accounting for most of the system's response variability. Given the threshold $C_{\min}$, N_d is set as the smallest integer such that [30]

$$\sqrt{\sum_{j=1}^{N_d} \lambda_j^2} \Big/ \sqrt{\sum_{j=1}^{n} \lambda_j^2} \geq C_{\min} \tag{3}$$

Here, $C_{\min} = 0.9$ so that the vectors $\boldsymbol{e}_j$ determining the domain are responsible for 90% of the overall variability. The reduced domain X_d is determined as

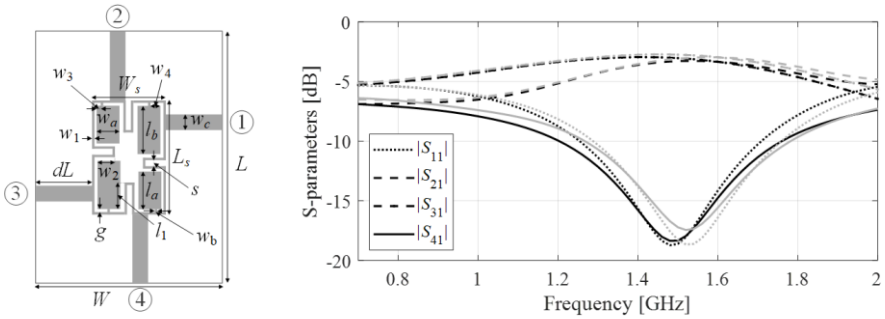

(a) (b)

Fig. 1. Multi-fidelity models: (a) exemplary miniaturized microstrip coupler, (b) frequency characteristics obtained with the low- and high-fidelity EM models $\boldsymbol{R}_c$ (gray) and $\boldsymbol{R}_f$ (black). The evaluation times for $\boldsymbol{R}_f$ and $\boldsymbol{R}_c$ are 210 and 90 seconds, respectively.

ICCS Camera Ready Version 2025
To cite this paper please use the final published version:
DOI: 10.1007/978-3-031-97632-2_7

$$X_d = \left\{ \boldsymbol{x} \in X : \boldsymbol{x} = \boldsymbol{x}_c + \sum_{j=1}^{N_d} a_j \boldsymbol{e}_j \right\} \cap X \tag{4}$$

The vector $\boldsymbol{x}_c = [\boldsymbol{l} + \boldsymbol{u}]/2$ (decision variable space center); a_j, $j = 1, \ldots, N_d$, are real numbers.

2.4 Global Search Stage

The first search step is global optimization using $\boldsymbol{R}_c$ and conducted in the reduced space X_d. It is a machine learning (ML) process with the infill criterion involving the improvement of the merit function . The underlying surrogate is kriging interpolation, which is optimized using the particle swarm optimizer (PSO).

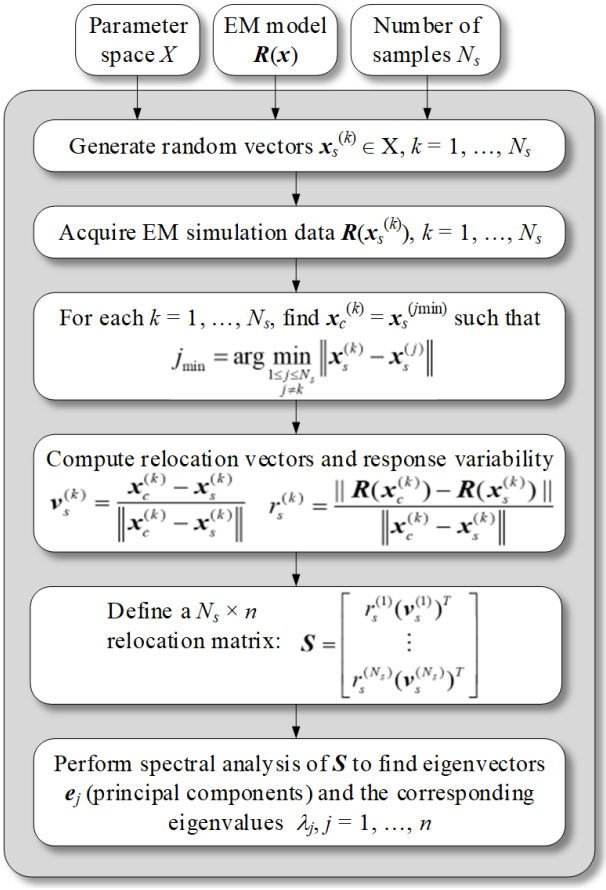

Fig. 2. The outline of RGSA [30]. The principal vectors $\boldsymbol{e}_j$ are associated with the directions significantly affecting the circuit outputs as quantified by the corresponding eigenvalues λ_j.

ICCS Camera Ready Version 2025
To cite this paper please use the final published version:
DOI: 10.1007/978-3-031-97632-2_7

The initial surrogate model is constructed using N_iN_d samples, where $N_i = 20$ in the verification experiments discussed in Section 3. The training points $\boldsymbol{x}_B^{(k)}$, $k = 1, \ldots, N_iN_d$, are allocated uniformly in the reduced domain X_d. A temporary surrogate $\boldsymbol{s}_{tmp}(\boldsymbol{x})$ is first built using $\{\boldsymbol{x}_B^{(k)}, \boldsymbol{R}_c(\boldsymbol{x}_B^{(k)})\}_{k = 1, \ldots, NiNd}$. Next, $\boldsymbol{s}_{tmp}$ is iteratively enhanced using the points produced by maximizing the mean square error (MSE) of the metamodel for $j = 1, 2, \ldots$

$$\boldsymbol{x}_B^{(N_iN_d+j)} = \arg\max_{\boldsymbol{x}\in X_d} MSE(\boldsymbol{s}_{tmp}(\boldsymbol{x})) \tag{5}$$

The infill vector is incorporated into the training dataset so that we have $\{\boldsymbol{x}_B^{(k)}, \boldsymbol{R}_c(\boldsymbol{x}_B^{(k)})\}_{k = 1, \ldots, NiNd + j}$. Maximization of MSE (here, using PSO) promotes the enhancement of the surrogate's accuracy. The model construction is terminated if the cross-validation-estimated relative RMS error becomes smaller than $E_{\max}$ (here, set to 20%) or the overall number of generated samples exceeds $2N_iN_d$. The final version of $\boldsymbol{s}_{tmp}(\boldsymbol{x})$ is renamed as the initial surrogate $\boldsymbol{s}^{(0)}(\boldsymbol{x})$.

Having $\boldsymbol{s}^{(0)}(\boldsymbol{x})$, the global search stage is launched within X_d, which is a machine learning (ML) algorithm. It starts by optimizing $\boldsymbol{s}^{(0)}$. Subsequent models, $\boldsymbol{s}^{(j)}$, $j = 1, 2, \ldots$, are obtained using the EM simulation results generated during the search. ML generates candidate solutions $\boldsymbol{x}^{(i+1)}$, $i = 0, 1, 2, \ldots$, by optimizing the cost function $U_S(\boldsymbol{x},\boldsymbol{s}^{(i)}(\boldsymbol{x}))$, i.e., using predicted improvement of the merit function. U_S coincides with the original merit function U (cf. Section 2.1) but it is computed based on $\boldsymbol{s}^{(i)}(\boldsymbol{x})$ rather than EM-simulated outputs. We have

$$\boldsymbol{x}^{(i+1)} = \arg\min_{\boldsymbol{x}\in X_d} U_S(\boldsymbol{x}, \boldsymbol{s}^{(i)}(\boldsymbol{x})) \tag{6}$$

Again, PSO acts as the core search engine, although any bio-inspired routine may be used. Note that because of the low cost of evaluating $U_S(\boldsymbol{x},\boldsymbol{s}^{(i)}(\boldsymbol{x}))$, solving of (6) may be executed using a high computational budget (here, 10,000 cost function calls). The candidate designs and the accumulated EM data are used to refine the surrogate: $\boldsymbol{s}^{(i)}(\boldsymbol{x})$ is built based on $\{\boldsymbol{x}_B^{(k)}, \boldsymbol{R}_c(\boldsymbol{x}_B^{(k)})\}_{k = 1, \ldots, 2NiNd + i}$, with $\boldsymbol{x}_B^{(2NiNd+i)} = \boldsymbol{x}^{(i)}$ for $i = 1, 2, \ldots$. The termination conditions are: $\|\boldsymbol{x}^{(i+1)} - \boldsymbol{x}^{(i)}\| < \varepsilon$ (convergence in argument), or no improvement in cost function for the last $N_{no\_improve}$ iterations. The parameter values utilized in the verification experiments are $\varepsilon = 10^{-2}$ and $N_{no\ improve} = 20$.

2.5 Fine Tuning

The global search stage is conducted in X_d using $\boldsymbol{R}_c$. Both factors enable significant computational savings. The same factors contribute to a degradation of reliability. This is rectified by adding a fine tuning stage, executed in the original decision variable space, and using high-fidelity EM analyzes. The underlying search routine is the trust-region (TR) algorithm [31]. The circuit response gradients are computed using finite differentiation (FD) [32]. Because the process starts from an already good design rendered by ML, the cost of final tuning is low. The algorithm is further expe-

ICCS Camera Ready Version 2025
To cite this paper please use the final published version:
DOI: 10.1007/978-3-031-97632-2_7

dited by replacing FD with a Broyden updating scheme [33], when the process approaches convergence, i.e., when $\|\boldsymbol{x}^{(i+1)} - \boldsymbol{x}^{(i)}\| < 10\varepsilon_{TR}$, where $\varepsilon_{TR} = 10^{-3}$ is the termination threshold.

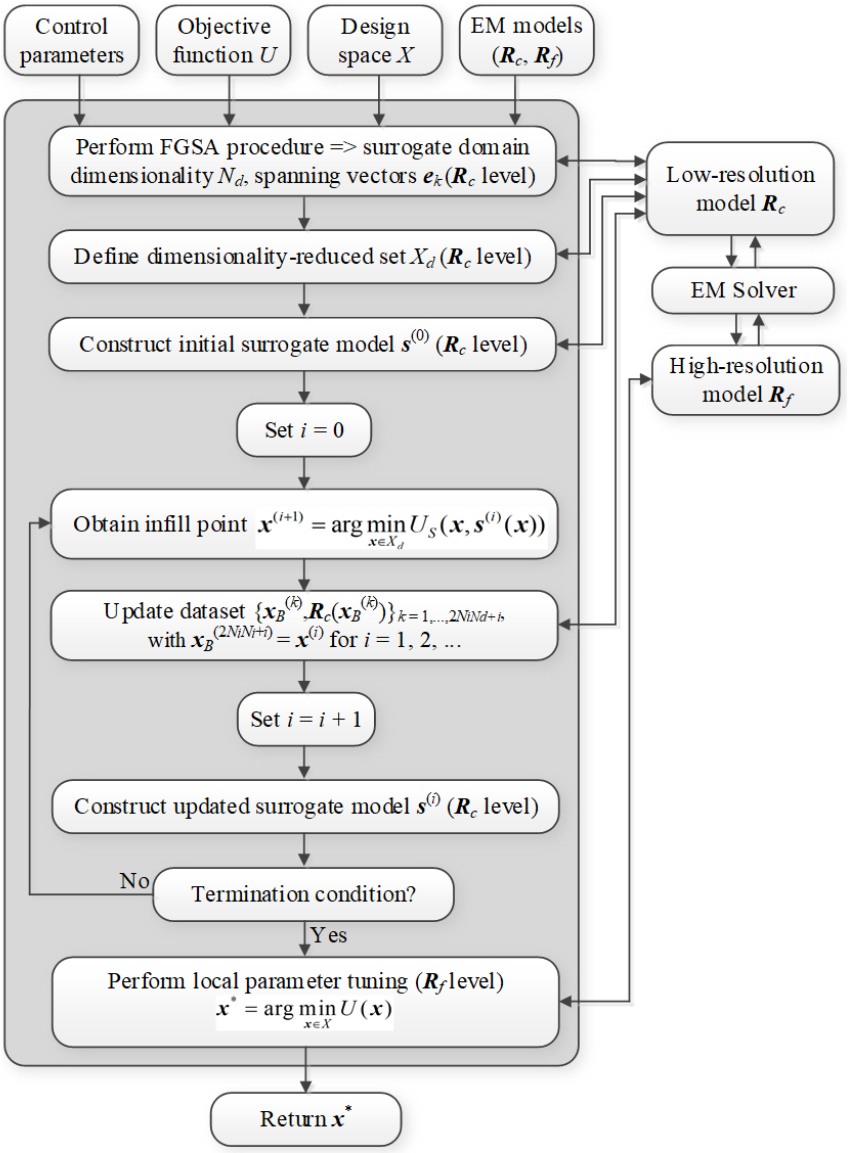

Fig. 3. Proposed machine learning procedure for global microwave optimization: flow diagram.

ICCS Camera Ready Version 2025
To cite this paper please use the final published version:
DOI: 10.1007/978-3-031-97632-2_7

2.6 Complete Algorithm

The complete optimization framework employs the algorithmic components discussed in Sections 2.2 through 2.5. Our approach utilizes fast surrogates built in a dimensionality-reduced space defined using RGSA. It should be reiterated that sensitivity analysis (RGSA) and the global search stage are conducted using the faster but less accurate low-fidelity EM model $\boldsymbol{R}_c$. Fine tuning is conducted using the high-fidelity model $\boldsymbol{R}_f$. There are few control parameters (N_r, N_i, $E_{\max}$, ε, $N_{no\_improve}$, ε_{TR}), all of which were discussed in detail in the preceding sections. None of these parameters is critical, and most control the resolution of the search process. The algorithm's flow diagram is illustrated in Fig. 3.

3 Results

This section showcases the operation of the suggested technique, demonstrated with two microstrip circuits and extensive comparisons to four benchmark methods, nature-inspired, gradient-based, and machine learning.

3.1 Test Circuits

Consider the test circuits illustrated in Fig. 4, and referred to as Circuits I and II. Their important parameters are listed in Table 1. CST Microwave Studio [36] is used to implement the computational models. The low-fidelity $\boldsymbol{R}_c$ model is a coarse-discretization version of the high-fidelity representation $\boldsymbol{R}_f$ (cf. Section 2.2). The resolution of $\boldsymbol{R}_f$ is determined through a grid convergence study. Note that both verification problems are challenging and require handling four distinct responses (matching, transmission, and isolation characteristics), several objectives, and carrying out the search in vast parameter spaces.

3.2 Setup

The setup of our framework and the benchmark procedures have been included in Table 2. There are four methods, including particle swarm optimizer (PSO) (Algorithm I) executed in two versions (500 and 1000 objective function evaluations), random-initialization gradient-based search (Algorithm II), and two ML routines. Among these, Algorithm III operates in the original parameter space. In contrast, Algorithm IV uses dimensionality reduction similar to that employed in this work, but the entire search process employs high-fidelity EM simulations. Observe that the budget assigned to Algorithm I is lower for bio-inspired methods yet considerable in absolute terms (a few days of CPU time). On the other hand, Algorithm II is incorporated to demonstrate the multimodality of our verification tasks.

3.3 Results

The results are displayed in Tables 3 and 4. The data encapsulates the mean value of the merit function and the optimization cost evaluated for ten independent executions of

ICCS Camera Ready Version 2025
To cite this paper please use the final published version:
DOI: 10.1007/978-3-031-97632-2_7

each method. Additionally, a success rate is displayed, which is the fraction of runs leading to satisfactory outcomes. The expenses are expressed in the equivalent number of $\boldsymbol{R}_f$ evaluations. Figures 5 and 6 show the circuit frequency characteristics for the selected runs of the suggested technique.

The main performance factors are reliability and computational efficiency. The reliability is assessed using the success rate, which is perfect (10/10) for our methodology and both test cases. In contrast, the benchmark techniques perform much worse. In particular, the fraction of successful runs for the random-start gradient search is only 5/10 and 8/10 for Circuit I and II, respectively, which underscores multimodality of the considered verification problems.

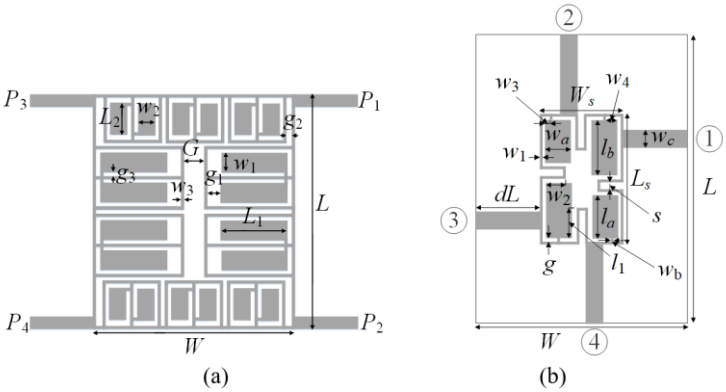

Fig. 4. Test cases: (a) Circuit I [34], (b) Circuit II [35].

Table 1. Essential data and design requirements for Circuits I and II

Parameter	Test case	
	Circuit I	Circuit II
Substrate	FR4 (ε_r = 4.4, h = 1.0 mm)	AD300 (ε_r = 2.97, h = 0.76 mm)
Design parameters[$]	$\boldsymbol{x} = [G\ g_1\ g_2\ g_3\ w_1\ w_3\ L_1\ L_2]^T$	$\boldsymbol{x} = [g\ l_{1r}\ l_a\ l_b\ w_1\ w_{2r}\ w_{3r}\ w_{4r}\ w_a\ w_b]^T$
Other parameters[$]	$L = 4w_1 + 10w_3 + 15g_3 + 2L_2$, $W = 4w_3 + 2L_1 + G + 2g_1 + 2g_3$	$L = 2dL+L_s$, $L_s = 4w_1+4g+s+l_a+l_b$, $W = 2dL + W_s$, $W_s = 4w_1+4g+s+2w_a$, $l_1 = l_b l_{1r}$, $w_2 = w_a w_{2r}$, $w_3 = w_{3r}w_a$, $w_4 = w_{4r}w_a$, w_c = 1.9 mm
EM model	CST Microwave Studio	CST Microwave Studio
$\boldsymbol{R}_c$ (low-fidelity)	~200,000 mesh cells Simulation time 70 s	~30,000 mesh cells Simulation time 90 s
$\boldsymbol{R}_f$ (high-fidelity)	~600,000 mesh cells Simulation time 320 s	~170,000 mesh cells Simulation time 210 s
Target frequencies [GHz]	f_0 = 1.0 GHz	f_0 = 1.5 GHz
Design goals	• Minimize $\lvert S_{11}\rvert$ and isolation $\lvert S_{41}\rvert$ at the operating frequency f_0 • Ensure power split ratio K_P = 0 dB	• Minimize matching $\lvert S_{11}\rvert$ and isolation $\lvert S_{41}\rvert$ at the operating frequency f_0 • Ensure power split ratio K_P = 0 dB
Parameter space X	$\boldsymbol{l} = [0.2\ 0.2\ 0.2\ 0.2\ 1.0\ 0.2\ 4.0\ 2.0]^T$ $\boldsymbol{u} = [1.5\ 1.5\ 1.5\ 1.0\ 3.5\ 0.5\ 12.0\ 8.0]^T$	$\boldsymbol{l} = [0.4\ 0.6\ 3\ 9\ 0.6\ 0.4\ 0.1\ 0.6\ 4.0\ 0.6]^T$ $\boldsymbol{u} = [0.5\ 0.85\ 6.5\ 11\ 0.95\ 0.7\ 0.4\ 0.9\ 5\ 0.7]^T$

[$] Dimensions in mm except for the relative ones (with subscript r), which are unitless.

ICCS Camera Ready Version 2025
To cite this paper please use the final published version:
DOI: 10.1007/978-3-031-97632-2_7

The performance of PSO is much better (9/10), yet not perfect, which is indicative of insufficient computational budget. On the other hand, the ML-based techniques match ours; however, they exhibit significantly higher computational expenses. The design quality measured by the objective function value is also highly competitive for the proposed approach. It is comparable to Algorithms III and IV but significantly better than Algorithms I and II. Also, one can note that increasing the budget for Algorithm I translates into a noticeable improvement in the results (by a few dB), which is another argument against direct EM-driven parameter tuning by means of bio-inspired techniques.

Computational efficiency is another advantage of the suggested technique. The average expenses incurred by the optimization process are below a hundred $\boldsymbol{R}_f$ evaluations, corresponding to 91 percent relative speedup over Algorithm I, 67 percent acceleration over Algorithm III, and 45 percent acceleration over Algorithm IV. At the same time, our method incurs costs comparable to gradient-based search (94 versus 54 EM simulations), which is remarkable given the local nature of Algorithm II. These benefits are the results of the mechanisms incorporated into the proposed framework, especially dimensionality reduction, the two-stage optimization process, and multi-fidelity EM analyses.

Table 2. Benchmark techniques

Algorithm	Algorithm type	Setup
This work	ML framework with dimensionality reduction	Control parameters: $N_r = 50$, $N_i = 20$, $E_{\max} = 20\%$, $\varepsilon = 10^{-2}$, $N_{no\_improve} = 20$, $\varepsilon_{TR} = 10^{-3}$ (the parameter's meaning has been explained in Section 2)
I	Particle swarm optimizer (PSO)	Swarm size $N = 10$, standard control parameters ($\chi = 0.73$, $c_1 = c_2 = 2.05$); the number of iterations set to 50 (ver. I) and 100 (ver. II)
II	Trust-region gradient-based optimizer	Random initial design, response gradients estimated using finite differentiation, termination criteria based on convergence in argument, and reduction of the trust region size [121]
III	Machine-learning procedure	Algorithm setup: • Initial surrogate set up to ensure relative RMS error not higher than 20% with the maximum number of training samples equal to 400; • Algorithm operates in the original parameter space (no dimensionality reduction); • Infill criterion: minimization of the predicted objective function.
IV	Machine-learning procedure	Algorithm setup: • The method is the same as the proposed one; however, the algorithm operates at the level of high-resolution EM models; • Control parameters: default values as in Table 1.

ICCS Camera Ready Version 2025
To cite this paper please use the final published version:
DOI: 10.1007/978-3-031-97632-2_7

Table 3. Circuit I: Optimization Results

Optimization algorithm	Performance figure		
	Average objective function value [dB]	Computational cost[$]	Success rate[#]
Algorithm I: PSO (50 iterations)	–20.8	500	9/10
Algorithm I: PSO (100 iterations)	–22.2	1,000	9/10
Algorithm II: Trust-region gradient-based algorithm	–7.5	49.0	5/10
Algorithm III: Machine learning operating in the original parameter space X	–26.2	449.8	10/10
Algorithm IV: Machine learning operating in the reduced space X_a; high-resolution model only	–24.5	183.6	10/10
Proposed algorithm	–25.0	66.0	10/10

[$] The cost expressed in terms of the number of EM simulations of the circuit under design.
[#] Number of runs at which the operating frequencies were allocated near the target frequency.

Table 4. Circuit II: Optimization Results

Optimization algorithm	Performance figure		
	Average objective function value [dB]	Computational cost[$]	Success rate[#]
Algorithm I: PSO (50 iterations)	–25.2	500	9/10
Algorithm I: PSO (100 iterations)	–29.1	1,000	9/10
Algorithm II: Trust-region gradient-based algorithm	–10.7	57.4	8/10
Algorithm III: Machine learning operating in the original parameter space X	–30.2	238.4	10/10
Algorithm IV: Machine learning operating in the reduced space X_a; high-resolution model only	–25.7	165.4	10/10
Proposed algorithm	–35.7	122.2	10/10

[$] The cost expressed in terms of the number of EM simulations of the circuit under design.
[#] Number of runs at which the operating frequencies were allocated near the target frequency.

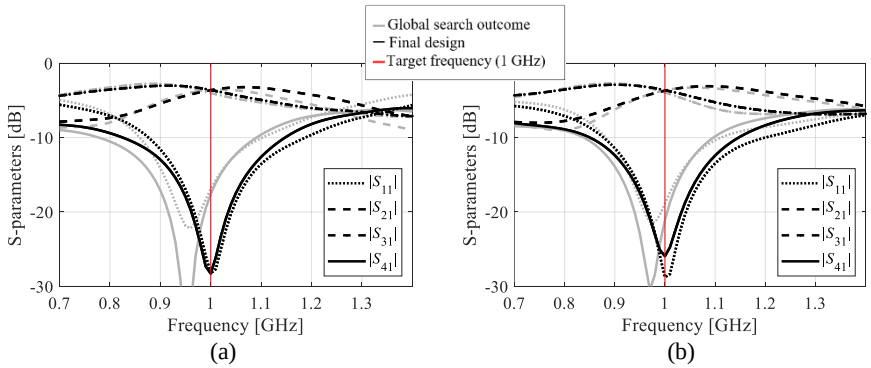

Fig. 5. Circuit I: designs found by the proposed multi-fidelity ML algorithm: (a) selected run 1, (b) selected run 2.

ICCS Camera Ready Version 2025
To cite this paper please use the final published version:
DOI: 10.1007/978-3-031-97632-2_7

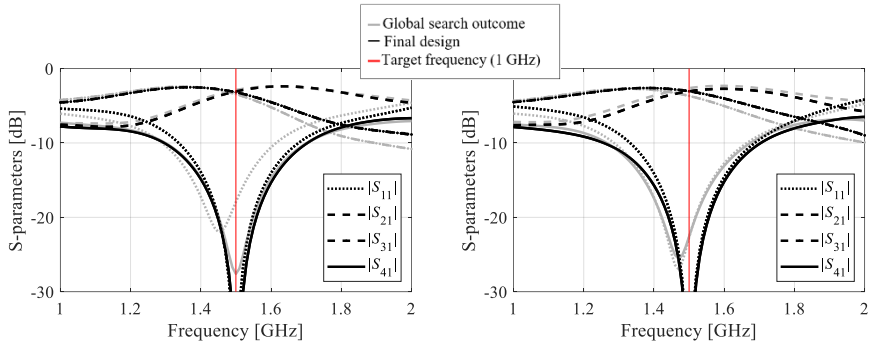

Fig. 6. Circuit II: designs found by the proposed multi-fidelity ML algorithm: (a) selected run 1, (b) selected run 2.

4 Conclusion

In this study, we developed an innovative methodology for the high-efficacy optimization of microwave passives. Our technique employs rapid global sensitivity analysis (RGSA) to determine a confined search domain (spanned by vectors responsible for the most significant changes in the system outputs) and a machine learning (ML) algorithm to execute global stage, complemented by gradient-based fine tuning. The efficiency is boosted by incorporating multi-fidelity EM simulations, low fidelity (faster but less accurate) for RGSA and ML, and high fidelity for final tuning. Combining these mechanisms results in competitive computational efficiency and reliability, as demonstrated by using two planer circuits and benchmarking against several state-of-the-art techniques.

Acknowledgment

The authors thank Dassault Systemes, France, for making CST Microwave Studio available. This work is partially supported by the Icelandic Centre for Research (RANNIS) Grant 239858 and by the National Science Centre of Poland Grant 2020/37/B/ST7/01448.

References

1. Liu, M., Lin, F., Two-section broadband couplers with wide-range phase differences and power-dividing ratio. IEEE Microwave Wireless Comp. Lett., **31**, 117–120 (2021)
2. Li, Q., Chen, X., Chi, P., Yang, T. Tunable bandstop filter using distributed coupling microstrip resonators with capacitive terminal. IEEE Microwave Wireless Comp. Lett., **30**, 35–38 (2020)
3. He, Z., Liu, C., A compact high-efficiency broadband rectifier with a wide dynamic range of input power for energy harvesting. **30**, 433–436 (2020)

ICCS Camera Ready Version 2025
To cite this paper please use the final published version:
DOI: 10.1007/978-3-031-97632-2_7

4. Zhou, J., Rao, Y., Yang, D., Qian, H.J., Luo, X. Compact wideband BPF with wide stopband using substrate integrated defected ground structur. IEEE Microwave Wireless Comp. Lett., **31**, 353–356 (2021)
5. Singh, H., Gupta, A., Kaler, R.S., Singh, S., Gill, J. Designing and analysis of ultrathin metamaterial absorber for W band biomedical sensing application. IEEE Sensors J., **22**, 10524–10531 (2022)
6. Koziel, S., Pietrenko-Dabrowska, A., Plotka P. Reduced-cost microwave design closure by multi-resolution EM simulations and knowledge-based model management. IEEE Access, **9**, 116326–16337 (2021)
7. Zhang, Z., Liu, B., Yu, Y., Cheng, Q.S. A microwave filter yield optimization method based on off-line surrogate model-assisted evolutionary algorithm. IEEE Trans. Microwave Theory Techn., **70**, 2925–2934 (2022)
8. Esmail, B.A.F., Koziel, S., Szczepanski, S., Majid H.A. Overview of approaches for compensating inherent metamaterials losses. IEEE Access, **10**, 67058–67080 (2022)
9. Liang, S., Fang, Z., Sun, G., Liu, Y., Qu, G., Zhang, Y. Sidelobe reductions of antenna arrays via an improved chicken swarm optimization approach. IEEE Access, **8**, 37664–37683 (2020)
10. Abdullah, M., Koziel, S., A novel versatile decoupling structure and expedited inverse-model-based re-design procedure for compact single-and dual-band MIMO antennas. IEEE Access, **9**, 37656–37667 (2021)
11. Jin, H., Zhou, Y., Huang, Y.M., Ding, S., Wu, K. Miniaturized broadband coupler made of slow-wave half-mode substrate integrated waveguide. IEEE Microwave Wireless Comp. Lett., **27**, 132–134 (2017)
12. Li, X., Luk, K.M., The grey wolf optimizer and its applications in electromagnetics. IEEE Trans. Ant. Prop., **68**, 2186–2197 (2020)
13. Oyelade, O.N., Ezugwu, A.E.-S., Mohamed, T.I.A., Abualigah L. Ebola optimization search algorithm: a new nature-inspired metaheuristic optimization algorithm. IEEE Access, **10**, 16150–16177 (2022)
14. Liu, F., Liu, Y., Han, F., Ban, Y., Jay Guo Y. Synthesis of large unequally spaced planar arrays utilizing differential evolution with new encoding mechanism and Cauchy mutation. IEEE Trans. Antennas Propag., **68**, 4406–4416 (2020)
15. Li, X., Guo, Y.-X., Multiobjective optimization design of aperture illuminations for microwave power transmission via multiobjective grey wolf optimizer. IEEE Trans. Ant. Prop., **68**, 6265–6276 (2020)
16. Li, W., Zhang, Y., Shi, X. Advanced fruit fly optimization algorithm. IEEE Access, **7**, 165583–165596 (2019)
17. Jiang, Z.J., Zhao, S., Chen, Y., Cui, T.J. Beamforming optimization for time-modulated circular-aperture grid array with DE algorithm. IEEE Ant. Wireless Propag. Lett., **17**, 2434–2438 (2018)
18. Cui, L., Zhang, Y., Jiao, Y. Robust array beamforming via an improved chicken swarm optimization approach. IEEE Access, **9**, 73182–73193 (2021)
19. Zhang, Z., Cheng, Q.S., Chen, H., Jiang F. An efficient hybrid sampling method for neural network-based microwave component modeling and optimization. IEEE Microwave Wireless Comp. Lett., **30**, 625–628 (2020)
20. Wu, Q., Wang, H., Hong W. Multistage collaborative machine learning and its application to antenna modeling and optimization. IEEE Trans. Ant. Propag., **68**, 3397–3409 (2020)

ICCS Camera Ready Version 2025
To cite this paper please use the final published version:
DOI: 10.1007/978-3-031-97632-2_7

21. Yu, X., Hu, X., Liu, Z., Wang, C., Wang, W., Ghannouchi, F.M. A method to select optimal deep neural network model for power amplifiers. IEEE Microwave Wireless Comp. Lett., **31**, 145–148 (2021)
22. Forrester, A.I.J., Keane, A.J. Recent advances in surrogate-based optimization. Prog. Aerospace Sci., **45**, 50–79 (2009)
23. Koziel, S., Pietrenko-Dabrowska, A. Performance-driven surrogate modeling of high-frequency structures. Springer, New York (2020)
24. Pietrenko-Dabrowska, A., Koziel, S., Expedited gradient-based design closure of antennas using variable-resolution simulations and sparse sensitivity updates. IEEE Trans. Ant. Propag., **70**, 4925–4930 (2022)
25. Pietrenko-Dabrowska, A., Koziel, S., Design centering of compact microwave components using response features and trust regions. Energies., **14**, 1–15 (2021)
26. Zhang, C., Feng, F., Gongal-Reddy, V., Zhang, Q.J., Bandler, J.W. Cognition-driven formulation of space mapping for equal-ripple optimization of microwave filters. IEEE Trans. Microwave Theory Techn., **63**, 2154–2165 (2015)
27. Bandler, J.W., Rayas-Sánchez, J.E., An early history of optimization technology for automated design of microwave circuits. IEEE J. Microwaves., **3**, 319–337 (2023)
28. Cervantes-González, J.C., Rayas-Sánchez, J.E., López, C.A., Camacho-Pérez, J.R., Brito-Brito, Z., Chávez-Hurtado, J.L. Space mapping optimization of handset antennas considering EM effects of mobile phone components and human body. Int. J. RF Microwave CAE., **26**, 121–128 (2016)
29. Ogurtsov, S., Koziel, S., Model management for cost-efficient surrogate-based optimization of antennas using variable-fidelity electromagnetic simulations. IET Microwaves Ant. Prop., **6**, 1643–1650 (2012)
30. Koziel, S., Pietrenko-Dabrowska, A., Leifsson L. Improved efficacy behavioral modeling of microwave circuits through dimensionality reduction and fast global sensitivity analysis. Sc. Rep., **14**, paper no. 19465 (2024)
31. Conn, A.R., Gould, N.I.M., Toint, P.L., Trust Region Methods, MPS-SIAM Series on Optimization (2000)
32. Levy, H., Lessman, F. Finite Difference Equations, Dover Publications Inc., New York (1992)
33. Broyden, C.G. A class of methods for solving nonlinear simultaneous equations. Math. Comp., **19**, 577–593 (1965)
34. Letavin, D.A., Shabunin, S.N., Miniaturization of a branch-line coupler using microstrip cells. Int. Scientific-Technical Conf. Actual Problems of Electronics Instrument Engineering (APEIE), 62–65 (2018)
35. Tseng, C., Chang, C., A rigorous design methodology for compact planar branch-line and rat-race couplers with asymmetrical T-structures. IEEE Trans. Microwave Theory Techn., **60**, 2085–2092 (2012)
36. CST Microwave Studio, ver. 2023, Dassault Systemes, France, 2023.

ICCS Camera Ready Version 2025
To cite this paper please use the final published version:
DOI: 10.1007/978-3-031-97632-2_7